Research Square

Preprints are preliminary reports that have not undergone peer review.
They should not be considered conclusive, used to inform clinical practice,
or referenced by the media as validated information.

Suction Sheaths Attenuate Both Intrarenal Temperature and Pressure During Pulsed Tm:YAG Laser Lithotripsy: A Bench-Top Study Using a Flexible Ureteroscope with Integrated Tip Sensors

Bo Lun Chiou
Kaohsiung Medical University
Khurshid R Ghani
University of Michigan
Yasser A. Noureldin
Northern Ontario School of Medicine University
Horacio Sanguinetti
Hospital de Clinicas. Buenos Aires
Pankaj N Maheshwari
Fortis Hospital Mulund
Daniele Castellani
LUM University
Murat Akand
Cankaya Yasam Hospital
John Michael DiBianco
The University of Florida
Smita De
Cleveland Clinic
Sung Yong Cho
Seoul National University College of Medicine, Seoul National University Hospital
Vineet Gauhar
Ng Teng Fong General Hospital
Brett Johnson
University of Texas Southwestern
Mohammad Hajiha
Emory University
Hsiang Ying Lee
ashum1009@hotmail.com

Kaohsiung Medical University Hospital, Kaohsiung Medical University

Research Article

Keywords:

Posted Date: August 28th, 2026

DOI: https://doi.org/10.21203/rs.3.rs-10513542/v1

License: This work is licensed under a Creative Commons Attribution 4.0 International License. Read Full License

Additional Declarations: No competing interests reported.

Abstract

Background

Laser lithotripsy during retrograde intrarenal surgery (RIRS) carries potential risks of thermal accumulation and elevated intrarenal pressure (IRP). This study aimed to compare the effects of different p-Tm:YAG laser settings and ureteral access sheath (UAS) configurations on intrarenal temperature (IRT) and IRP.

Methods

This *in vitro* study utilized a simulation model to evaluate four distinct pulsed Thulium:YAG (p-Tm:YAG) laser configurations: 1.0 J × 10 Hz, 10 W;0.6 J × 20 Hz, 12 W;1.0 J × 20 Hz, 20 W;0.4 J × 50 Hz, 20 W. These settings were cross-tested using C-UAS (conventional ureteral access sheaths; UAS; Cook, 10.7/12.7 Fr and 12/14 Fr) and FANS (Flexible and Navigable Suction ureteral access sheath, Innovex, 10/12 Fr and 11/13 Fr). Both IRT and IRP were continuously monitored using a flexible ureteroscope equipped with distal-tip sensors, and measurements were recorded at 10-second intervals throughout the lasing process.

Results

Active suction substantially mitigated both IRT and IRP elevation compared to conventional UAS. Temperature-time regression lines showed the 20-W settings produced faster temperature increases than the 10-W settings. Among all tested configurations, the larger suction sheath (FANS; 11/13 Fr) consistently maintained the most stable thermal and pressure environments, whereas smaller sheath diameters amplified both responses across all lasing conditions. Furthermore, under active suction, IRP showed no consistent time-dependent cumulative trend; instead, intermittent pressure fluctuations may have been more closely related to transient outflow obstruction during fragment evacuation than to elapsed experimental time.

Conclusion

In this in vitro RIRS model, smaller sheath diameters were associated with higher intrarenal temperature and pressure, while suction sheaths effectively reduced both IRT and IRP. Thermal elevation was more evident at higher laser power, and different energy–frequency settings produced distinct thermal profiles despite equivalent total power. IRP showed no consistent time-dependent cumulative trend under standardized conditions with a non-restrictive lumen. These findings highlight the importance of simultaneous IRT and IRP monitoring and suggest that suction sheaths, particularly when combined with pressure- and temperature-sensing ureteroscopes, may enhance the safety of flexible ureteroscopy.

1.Introduction

Retrograde intrarenal surgery (RIRS) with high-power lasers raises important thermal and pressure-related safety concerns within the renal microenvironment. Thermally, 91–96% of laser energy is converted to heat during lithotripsy [1]. At 43°C, tissue damage has been associated with exposure times of 120 minutes [2]. Although high-flow irrigation is commonly used to limit heat buildup, it can create a “cooling–pressure dilemma” [3–5].

Excessive irrigation may increase intrarenal pressure (IRP) beyond the safe threshold of 40 cm H2O (29 mmHg), potentially leading to pyelovenous backflow, parenchymal injury, and postoperative urosepsis [4, 5]. To address these combined risks, suction ureteral access sheaths such as the Flexible and Navigable Suction (FANS) sheath have been introduced into clinical practice and have been increasingly adopted in contemporary RIRS [6, 7]. However, the combined thermal and pressure effects of pairing these technologies have not been studied well.

FANS were developed to improve outflow by actively removing irrigation fluid and stone debris while maintaining a more stable, low-pressure pelvicalyceal environment [6–8]. In theory, improved outflow may help reduce both intrarenal temperature (IRT) and IRP during laser activation. However, these effects may vary according to sheath design, sheath diameter, irrigation dynamics, and laser settings. This uncertainty is particularly relevant as surgeons increasingly attempt to treat larger stone burdens using high-power laser platforms and different lasing techniques, where the balance among visibility, efficiency, thermal safety, and pressure control becomes central to procedural safety [8–10].

We therefore conducted a bench-top study using a ureteroscope with integrated tip sensors to test the hypothesis that FANS mitigates intrarenal temperature elevation and stabilizes intrarenal pressure during pulsed Tm:YAG lithotripsy, particularly at higher-power settings.

2.Material and Methods

2.1 Study design:

This was an in vitro experimental study. To improve reproducibility and reduce inter-operator variability, all procedures, including laser parameter adjustment, UAS exchange, and real-time data collection, were performed by a single trained investigator. To increase reliability and reduce random experimental error, each standardized lithotripsy protocol was performed in triplicate within each cohort. Cohorts were stratified by laser modulation strategy and UAS configuration, including sheath size and type (conventional, marked as C-UAS vs. FANS), to assess their independent and combined effects on intrarenal temperature and pressure dynamics.

2.2 Experimental Setup:

An in vitro upper urinary tract model was established to evaluate intrarenal pressure and temperature changes during laser activation. A kidney–ureter–bladder silicone model was placed in a water-filled container to simulate the urinary tract environment (Fig. 1A-B). The internal anatomy of the model was constructed using real human renal CT scan data, providing a realistic representation of the collecting system, ureter, and bladder. The silicone material closely mimics the appearance and tactile characteristics of the urinary tract, allowing the experimental setting to approximate clinical ureteroscopic procedures. The model was watertight, with all external walls and connections sealed to prevent fluid leakage during irrigation and suction.

Continuous irrigation was delivered through a fixed irrigation system (Hystero Pump II, Richard Wolf, Knittlingen, Germany) positioned on the right side of the setup, allowing a constant inflow rate throughout the experiment (Fig. 1C). Throughout all experiments, the irrigation pressure was consistently maintained at 100 mmHg. A suction pump (DF-506K Portable Suction Unit, DOCTOR'S FRIEND MEDICAL INSTRUMENT CO., LTD. Taiwan), positioned on the left side, was connected to the FANS when suction mode was applied (Fig. 1D).

The flexible ureteroscope HAWK Video Uretero-Renoscope System (Hangzhou Hawk Optical Electronic Instruments CO., LTD., China) was used. This scope has an 8.5-Fr distal tip and insertion shaft, with a working length of 670 mm. The working channel measures 3.6 Fr, allowing the passage of laser fibers and ancillary instruments during the experiment. HAWK scope is equipped with sensors positioned at the distal tip allowing continuous monitoring of IRT (°C) and IRP (mmHg) to capture the dynamic response of the environment. Real-time IRT and IRP measurements were recorded and displayed on the monitor during the experiment. (Fig. 2)

2.2.1 *Lasing System and Fragmentation Strategies*

A solid-state p-Tm:YAG laser system (Dornier Thulio® YAG laser, Dornier MedTech, Germany), fiber size 270um, was employed for all lithotripsy trials. To investigate the interplay between pulse energy and frequency on in vitro environment, four distinct lasing settings were compared and denoted below. We aimed to select four commonly used settings including 1.0J × 10 Hz (Total Power:10W), 0.6J × 20 Hz (Total Power:12W), 1.0J × 20 Hz (Total Power: 20W) and 0.4J × 50 Hz (Total Power: 20W).

In each trial, a standardized solid spherical plaster stone, 12 mm in diameter made by Dornier (Dornier Medical Systems, Germering, Germany) was placed within the renal pelvis. Continuous lasing was performed for 60 seconds to simulate a maximal thermal load scenario, aiming to fragment the stone into dust or fragments. Before each experimental run, the temperature was reduced to 20°C at fluid temperature to ensure that all experiments started from the same baseline temperature at 0 second.

2.2.2 *UAS and suction setting*

To assess the impact of sheath dimensions and suction capability, four UAS configurations were tested. C-UAS (Cook Medical) included 10.7/12.7 Fr and 12/14 Fr sizes, while FANS sheath (Innovex) included 10/12 Fr and 11/13 Fr sizes. In experiments using the FANS sheath, suction pressure was maintained at a suction pressure of 100 mmHg. IRT and IRP were continuously monitored during laser activation to assess the effects of laser settings, sheath size, and sheath type on thermal and pressure dynamics. This setup was specifically designed to isolate and quantify the net thermal accumulation (ΔT) generated by different p-Tm: YAG laser settings, effectively eliminating potential confounding variables arising from ambient temperature fluctuations.

2.3 Analysis

The primary aim of analysis was the temporal relationship between laser application and the resulting variations in temperature and pressure inside the artificial kidney. IRT and IRP measurements were analyzed separately according to C-UAS or FANS, UAS size, and energy setting (J and Hz). For each experimental condition, measurements were obtained every 10 seconds for a total of 60 seconds.

To characterize temporal changes, simple linear regression models were fitted for each experimental condition using time as the independent variable and IRT or IRP as the dependent variable:

$Y = \beta 0 + \beta 1 \times time$

where β0 represents the baseline value and β1 represents the rate of change over time (slope). Slopes were expressed per 10 seconds to facilitate interpretation of thermal and pressure dynamics.

For temperature analysis, the primary outcome was the slope of temperature increase over time. Additional descriptive indices included baseline temperature (0 sec), final temperature (60 sec), total temperature change (ΔIRT). Experimental conditions were descriptively compared according to UAS type (Conventional/ FANS), UAS size, and energy setting. IRP was analyzed using the same regression framework. However, because pressure measurements demonstrated substantial variability and inconsistent temporal patterns, IRP analyses were interpreted primarily descriptively.

For groups where temperature or pressure stabilized before the end of the 60-second period, we defined it as a steady plateau value. Each C-UAS/ FANS–UAS size–energy combination was tested in triplicate. Because the three replicates per condition were averaged before fitting, run-to-run variability could not be estimated; we therefore report regression slopes as descriptive measures of effect size and do not report R-squared, which would reflect only the linear fit of averaged data. Formal inferential statistical testing and p-value–based comparisons were not performed. Instead, analyses focused on effect-size estimation, including regression slopes and total changes over time. Data management and statistical analysis were performed using SAS software, version 9.4 (SAS Institute Inc., Cary, NC, USA).

3.Results

3.1 Temperature Dynamics

The baseline experimental configurations are summarized in Table 1, which presents temperature slopes across four laser settings and four UAS configurations. Temperature increased linearly over time in all experimental settings. The fitted models were stable across groups. In addition, steeper temperature increases per 10-second interval corresponded to greater total temperature elevation, indicating consistency between the rate of warming and the overall thermal change.

Table 1
Summary of IRT Slopes Across Different UAS Configurations and Laser Settings

Variables	Baseline IRT,0 sec(°C)	Final IRT,60 sec(°C)	Delta IRT	Slope per 10 seconds (°C/10s)	Regression equation
C-UAS, size:12/14 Fr., 1J x 10 Hz	20.1333	23.2667	3.13333	0.48333	IRT = 20.445°C + 0.0483°C * time_sec
C-UAS, size:12/14 Fr., 0.6 J x 20Hz	20.0000	23.4667	3.46667	0.54881	IRT = 20.230°C + 0.0549°C * time_sec
C-UAS, size:12/14 Fr., 1.0 J x 20Hz	20.0000	26.4667	6.46667	0.97143	IRT = 20.681°C + 0.0971°C * time_sec
C-UAS, size:12/14 Fr., 0.4 J x 50Hz	20.1000	29.8333	9.73333	1.46905	IRT = 21.912°C + 0.1469°C * time_sec
C-UAS, size:10.7/12.7 Fr., 1J x 10 Hz	20.0000	23.2667	3.26667	0 .52024	IRT = 20.292°C + 0.0520°C * time_sec
C-UAS, size:10.7/12.7 Fr., 0.6 J x 20Hz	20.0000	24.6667	4.66667	0.74762	IRT = 20.086°C + 0.0748°C * time_sec
C-UAS, size:10.7/12.7 Fr., 1.0 J x 20Hz	20.0000	26.1000	6.10000	0.99167	IRT = 20.392°C + 0.0992°C * time_sec
C-UAS, size:10.7/12.7 Fr., 0.4 J x 50Hz	20.0000	25.4333	5.43333	0.83571	IRT = 20.760°C + 0.0836°C * time_sec
FANS, size:11/13 Fr., 1J x 10 Hz	20.0000	21.6000	1.60000	0.21071	IRT = 20.482°C + 0.0211* time_sec
FANS, size:11/13 Fr., 0.6 J x 20Hz	20.0000	21.6000	1.60000	0.25238	IRT = 20.414°C + 0.0252°C * time_sec
FANS, size:11/13 Fr.,	20.0000	23.3667	3.36667	0.49167	IRT = 20.668°C + 0.0492°C * time_sec

*IRT, Intrarenal temperature; FANS, Flexible and Navigable Suction sheath; C-UAS, Conventional UAS; UAS, ureteral access sheath

Variables	Baseline IRT,0 sec(°C)	Final IRT,60 sec(°C)	Delta IRT	Slope per 10 seconds (°C/10s)	Regression equation
1.0 J x 20Hz					
FANS, size:11/13 Fr., 0.4 J x 50Hz	20.0000	22.1000	2.10000	0.35833	IRT = 20.873°C + 0.0358°C * time_sec
FANS, size: 10/12 Fr., 1J x 10 Hz	20.0000	23.1333	3.13333	0.47500	IRT = 20.404°C + 0.0475°C * time_sec
FANS, size: 10/12 Fr., 0.6 J x 20Hz	20.0000	23.2000	3.20000	0.54405	IRT = 20.287°C + 0.0544°C * time_sec
FANS, size: 10/12 Fr., 1.0 J x 20Hz	20.0000	26.2333	6.23333	1.01190	IRT = 20.569°C + 0.1012°C * time_sec
FANS, size: 10/12 Fr., 0.4 J x 50Hz	20.0000	25.1333	5.13333	0.85476	IRT = 20.579°C + 0.0855°C * time_sec
*IRT, Intrarenal temperature; FANS, Flexible and Navigable Suction sheath; C-UAS, Conventional UAS; UAS, ureteral access sheath					

Figure 3 shows the temperature-time regression lines for different laser settings under identical hardware conditions. The 20-W settings produced faster temperature increases than the 10-W settings. In the C-UAS 12/14 Fr configuration, laser setting 1.0 J × 20 Hz and laser setting 0.4 J × 50 Hz had the same total power output (20 W) but markedly different heating rates (0.97°C vs. 1.47°C per 10 seconds, respectively; Table 1). This finding suggests that thermal change may depend not only on total power, but also on the energy delivery mode. At lower power settings (10–12 W), the difference in heating rate between laser setting 1.0 J × 10 Hz and laser setting 0.6 J × 20 Hz was relatively small, and the higher-energy, lower-frequency setting showed the steeper slope.

Supplementary Fig. 1 further indicates that UAS clearance space influences local thermal dynamics. In the group, the temperature-time regression lines became steeper as UAS size decreased, indicating faster temperature elevation with smaller sheath sizes. In contrast, under the 0.4 J × 50 Hz setting in the C-UAS group, the larger 12/14 Fr sheath showed a greater temperature rise than the smaller 10.7/12.7 Fr sheath.

Supplementary Fig. 2 compares temperature-time regression lines across UAS configurations within each laser setting. Regardless of the energy configuration, the FANS 11/13 Fr configuration consistently showed the flattest and most stable temperature rise. Under the 0.4 J × 50 Hz setting, the C-UAS with 12/14 Fr. size showed a noticeably greater rise in temperature, whereas the FANS with 11/13 Fr. maintained a smoother and more controlled upward trend. These findings suggest that the FANS with 11/13 Fr. provides the most predictable thermal environment across different lasing conditions.

3.2 Pressure Dynamics

Unlike the strongly linear temperature profiles, intrarenal pressure (IRP) did not show a clear linear relationship over time. Table 2 summarizes the associations among time, pressure dynamics, laser settings, UAS type, and UAS size.

Table 2
Summary of IRP Slopes Across Different UAS Configurations and Laser Settings

Variables	Baseline IRP at 0 sec(mmHg)	Final IRP at 60 sec(mmHg)	Delta IRP(mmHg)	Slope per 10 seconds (mmHg/10s)	Regression equation
C-UAS, size:12/14 Fr., 1J x 10 Hz	-2.33333	-1.33333	1.00000	0.08333	IRP =-1.964mmHg + 0.0083 mmHg* time_sec
C-UAS, size:12/14 Fr., 0.6 J x 20Hz	-0.66667	-1.00000	-0.33333	-0.07143	IRP =-0.643 mmHg + -0.0071 mmHg * time_sec
C-UAS, size:12/14 Fr., 1.0 J x 20Hz	-0.33333	-0.66667	-0.33333	− .09524	IRP =-0.524 mmHg +-0.0095 mmHg * time_sec
C-UAS, size:12/14 Fr., 0.4 J x 50Hz	-0.66667	-0.33333	0.33333	0.07143	IRP =-0.786 mmHg + 0.0071 mmHg * time_sec
C-UAS, size:10.7/12.7 Fr., 1J x 10 Hz	7.33333	7.00000	-0.33333	-0.02381	IRP = 7.119 mmHg +-0.0024 mmHg * time_sec
C-UAS, size:10.7/12.7 Fr., 0.6 J x 20Hz	6.33333	8.66667	2.33333	0.30952	IRP = 6.690 mmHg + 0.0310 mmHg * time_sec
C-UAS, size:10.7/12.7 Fr., 1.0 J x 20Hz	7.00000	8.33333	1.33333	0.21429	IRP = 7.071 mmHg + 0.0214 mmHg * time_sec
C-UAS, size:10.7/12.7 Fr., 0.4 J x 50Hz	7.00000	6.66667	-0.33333	-0.04762	IRP = 7.000 mmHg +-0.0048 mmHg * time_sec
FANS, size:11/13 Fr., 1J x 10 Hz	-3.66667	-3.00000	0.66667	0.16667	IRP=-3.881mmHg + 0.0167mmHg* time_sec
FANS, size:11/13 Fr., 0.6 J x 20Hz	-3.00000	-3.00000	0.00000	0.09524	IRP=-3.476mmHg + 0.0095mmHg* time_sec

*IRP, Intrarenal pressure; FANS, Flexible and Navigable Suction sheath; C-UAS, Conventional UAS; UAS, ureteral access sheath

Variables	Baseline IRP at 0 sec(mmHg)	Final IRP at 60 sec(mmHg)	Delta IRP(mmHg)	Slope per 10 seconds (mmHg/10s)	Regression equation
FANS, size:11/13 Fr., 1.0 J x 20Hz	-2.66667	-2.33333	0.33333	0.05952	IRP=-2.702mmHg + 0.0060mmHg* time_sec
FANS, size:11/13 Fr., 0.4 J x 50Hz	-3.00000	-2.66667	0.33333	0.04762	IRP=-2.857mmHg + 0.0048mmHg* time_sec
FANS, size:10/12 Fr., 1J x 10 Hz	0.33333	-1.00000	-1.33333	-0.64286	IRP = 2.738mmHg+-0.0643mmHg* time_sec
FANS, size:10/12 Fr., 0.6 J x 20Hz	-1.00000	-1.00000	0.00000	0.00000	IRP=-1.000mmHg + 0.0000mmHg* time_sec
FANS, size:10/12 Fr., 1.0 J x 20Hz	-1.00000	-1.00000	0.00000	0.02381	IRP=-1.119mmHg + 0.0024mmHg * time_sec
FANS, size:10/12 Fr., 0.4 J x 50Hz	-1.33333	1.00000	2.33333	0.45238	IRP=-1.452mmHg + 0.0452mmHg* time_sec

*IRP, Intrarenal pressure; FANS, Flexible and Navigable Suction sheath; C-UAS, Conventional UAS; UAS, ureteral access sheath

Figure 4 shows the pressure-time regression lines across laser settings while controlling for UAS type and size. In the C-UAS groups, IRP remained essentially flat over time, with no meaningful linear trend across settings. Both the larger lumen (12/14 Fr) and smaller lumen (10.7/12.7 Fr) configurations produced nearly horizontal regression lines, indicating that pressure did not progressively accumulate during the 60-second activation period under passive drainage. In the FANS sheath group, the 11/13 Fr configuration consistently showed flat slopes near or below zero across all lasing modes, indicating a stable and predictable pressure profile.

When UAS size was examined as the primary variable (Supplementary Fig. 3), IRP tended to be higher with smaller sheaths than with larger sheaths in both C-UAS and FANS modes. Across most energy settings, however, the pressure-time regression lines showed non-linear fluctuations rather than consistent temporal trends for both sheath types.

When laser energy settings (J × Hz) were analyzed as the primary variable under controlled hardware conditions (Supplementary Fig. 4), no clear linear or sequential pattern in pressure slopes was observed across laser modes. The smaller C-UAS was associated with the highest intrarenal pressure, but IRP did not vary markedly across energy settings.

4.Discussion

This study characterized the dynamic IRT and IRP responses during p-Tm:YAG lithotripsy using a standardized 1.2 cm artificial stone model. Three principal findings emerged. First, active suction with FANS attenuated thermal accumulation and stabilized IRP under the tested conditions, suggesting that suction-assisted fluid management may help balance thermal safety and pressure stability. Second, thermal accumulation was not determined by total laser power alone. At matched 20 W output, higher pulse energy appeared to be the predominant factor associated with greater thermal accumulation in most configurations, whereas the high-frequency 20 W (0.4 J × 50 Hz) setting produced a steeper thermal rise in the C-UAS 12/14 Fr configuration without suction. Third, under FANS, IRP did not follow a simple time-cumulative pattern but fluctuated nonlinearly, suggesting that pressure behavior may be influenced by intermittent outflow obstruction during fragment or dust evacuation. Together, these findings indicate that thermal and pressure responses during p-Tm:YAG lithotripsy are shaped by the interaction among laser energy delivery, UAS configuration, irrigation flow, suction efficiency, and outflow conditions.

The finding that active suction with FANS attenuated thermal accumulation and stabilized IRP should be interpreted in the context of the recognized temperature–pressure trade-off during flexible ureteroscopy. High irrigation flow may reduce laser-induced heat accumulation, but excessive irrigation may increase IRP if outflow is insufficient or not actively regulated [3, 4, 8–10]. This pressure component is clinically relevant because elevated IRP during flexible ureteroscopy has been associated with pyelovenous backflow, infection-related complications, and renal injury, and prior reviews have emphasized the importance of maintaining low intrarenal pressure during endourological procedures [3, 4, 8]. In this regard, suction-assisted systems may provide a more favorable fluidic environment by enhancing fluid egress while preserving irrigation-mediated heat dissipation [8–10]. This balance is particularly important because stone-containing models may produce greater thermal rise and ureteroscope-tip measurements may underestimate actual localized intracaliceal peak temperatures. Hein et al. demonstrated that stone-containing models produced a greater and more turbulent temperature rise than blank water models [11], while Okhunov et al. showed that scope-tip measurements were substantially lower than true intracaliceal temperatures [12], and Yang et al. further demonstrated that temperatures adjacent to the laser fiber tip were significantly higher than temperatures recorded by a temperature-monitoring ureteroscope [13]. Therefore, the ability of active suction to reduce thermal accumulation while stabilizing IRP may have practical safety implications in this experimental kidney model, especially during continuous laser activation.

At matched 20 W output, the present findings suggest that higher pulse energy appeared to be the predominant factor associated with greater thermal accumulation in most configurations. The 20 W setting with higher pulse energy, 1.0 J × 20 Hz, generally produced slightly greater thermal accumulation than the 20 W high-frequency setting, 0.4 J × 50 Hz, except in the C-UAS 12/14 Fr configuration without suction. In that specific configuration, the high-frequency 20 W setting, 0.4 J × 50 Hz, produced a steeper thermal rise than 1.0 J × 20 Hz, suggesting that pulse frequency may play an important role in accelerating thermal accumulation under selected outflow conditions. This observation is consistent with Hein et al., who reported higher end temperatures at higher frequencies at a given power output [11]. However, because this frequency-related effect was not reproduced across the smaller C-UAS 10.7/12.7 Fr group or the FANS cohorts, it should not be interpreted as a universal frequency effect. Prior thermal studies have consistently shown that laser power, pulse modulation, irrigation flow, and procedural conditions influence temperature behavior during ureteroscopic lithotripsy [11, 14–17]. Therefore, the present results suggest that total laser power alone does not predict thermal propagation; instead,

thermal behavior appears to depend on the interaction among pulse energy, pulse frequency, irrigation flow, sheath geometry, suction efficiency, and outflow conditions.

Under active suction, IRP behavior appeared to be governed less by cumulative lasing time than by intermittent outflow dynamics. The lack of a consistent time-dependent pressure trend across most FANS cohorts suggests that pressure fluctuations did not follow a simple cumulative pattern. Instead, abrupt pressure spikes may reflect transient narrowing of the effective outflow pathway during fragment or dust evacuation. This interpretation is supported by prior clinical observations that small stone fragments can accumulate between the scope and suction sheath, impair irrigation reflux even under negative-pressure suction, and contribute to elevated IRP [18]. The pressure pattern observed with the restricted-lumen FANS 10/12 Fr configuration may be consistent with this proposed outflow-bottleneck mechanism. Under the high-frequency 20 W setting, 0.4 J × 50 Hz, rapid generation of fine stone dust and suspended particulate debris may have increased outflow resistance, producing a highly linear pressure rise. By contrast, under the 10 W setting, 1.0 J × 10 Hz, the longer inter-pulse interval may have allowed more effective evacuation of residual debris, resulting in a negative pressure slope. These findings are consistent with the concept that dusting and fragmenting strategies can influence stone dust burden, visualization, evacuation efficiency, and IRP behavior during ureteroscopic lithotripsy [19]. Therefore, in suction-assisted systems, the principal pressure-related risk may shift from prolonged laser activation itself to transient fragment- or dust-related bottlenecks, highlighting the importance of maintaining effective outflow during active lithotripsy.

Several limitations should be acknowledged. First, this in vitro model does not reproduce the biological heat-sink effect of renal blood flow and may therefore overestimate thermal accumulation compared with in vivo conditions [1, 9]. Although the baseline temperature was standardized at 20°C for experimental consistency, a clinical starting temperature of 37°C would shorten the time required to reach the thermal injury threshold of 43°C [2]. Second, the model does not capture the biological and biomechanical complexity of the urothelium and submucosa. In clinical practice, continuous active negative pressure (100 mmHg) may cause mucosal suction injury or transient collapse of the collecting system, altering fluid dynamics and drainage efficiency in ways not reflected by this rigid setup. To reduce confounding, however, both irrigation and suction pressures were kept constant throughout the experiments. Third, artificial stones may not fully replicate the thermal conductivity, structural heterogeneity, and fragmentation behavior of natural stones. Fourth, our findings are only reflective of one laser and need to be verified with other pulse modulated lasers. Fifth, fragment-related obstruction was inferred from pressure behavior rather than directly visualized or quantified; therefore, the proposed bottleneck mechanism should be interpreted as hypothesis-generating. Finally, because intrarenal temperature was measured at the scope tip, peak temperatures at the laser–stone interface were likely higher than recorded [1, 12, 13]. Despite these limitations, the study provides a controlled comparative analysis of the pressure and thermal effects of different p-Tm:YAG lasing strategies.

The present findings have several practical implications for RIRS. Active suction through a FANS sheath may help address the classical “temperature–pressure trade-off” by reducing thermal accumulation while maintaining a more stable IRP profile during laser lithotripsy. Thermal behavior should not be judged by total laser power alone, because pulse energy, pulse frequency, sheath geometry, suction efficiency, and outflow conditions interact to determine the rate of temperature rise. In clinical practice, sheath selection should therefore be individualized according to the anticipated stone burden, expected dust or fragment load, and planned lasing strategy. Smaller sheath diameters may amplify both thermal and pressure responses, whereas the larger suction sheath

configuration tested in this study, particularly the 11/13 Fr FANS, provided the most stable thermal and pressure environment. These observations suggest that larger FANS sheaths may be favorable for complex, prolonged, or high-burden RIRS procedures when anatomically feasible. In addition, because ureteroscope tip measurements may underestimate localized peak temperatures near the laser–stone interface, real-time monitoring of both IRT and IRP may provide an additional safety layer and help guide intraoperative decisions regarding irrigation, suction, lasing duration, and temporary pauses. Future studies should validate these bench-top findings in vivo, where renal blood flow, tissue compliance, collecting system dynamics may substantially influence both temperature and pressure behavior. In addition, these findings should be tested across other laser platforms, different pulse-modulation technologies, irrigation settings, suction pressures to determine whether the observed interaction remains consistent across different operative environments.

Conclusion

In this in vitro study, smaller sheath diameters were associated with parallel increases in temperature and pressure, whereas suction sheaths reduced both IRT and IRP. Temperature rise became more pronounced at higher power, and distinct energy-frequency settings produced different thermal responses even at the same total power, especially at higher-power settings. In most standardized RIRS scenarios with a non-restrictive lumen, IRP showed no consistent time-dependent cumulative trend. These findings support simultaneous monitoring of IRT and IRP and suggest pairing suction-enabled access sheaths with real-time intrarenal sensing as a candidate safety strategy for high-power flexible ureteroscopy, pending in vivo validation.

Declarations

Ethics declaration:

Not applicable. This bench-top study did not involve human participants, human tissue, or animals.

Funding:

The authors received no specific funding for this work.

Acknowledgements

The authors thank the help from the Division of Medical Statistics and Bioinformatics, Department of Medical Research, Kaohsiung Medical University Hospital, Kaohsiung Medical University.

Author Contribution

H.Y.L. conceived the study idea and supervised the project. B.L.C. wrote the original manuscript draft and coordinated manuscript revision. B.L.C. and H.Y.L. developed the hypotheses and interpretation presented in the Discussion. K.R.G., Y.A.N., H.S., P.N.M., D.C., M.A., J.M.D., S.D., S.Y.C., V.G., B.J., and M.H. provided expert input, interpretation of the findings, and critical revision of the manuscript. All authors reviewed and approved the final manuscript.

References

1. Kim J, Hong SH (2025) Rise in intraluminal temperature during ureteroscopy: Is this a concern? Investig Clin Urol 66:1–10. 10.4111/icu.20240369
2. Pauchard F, Corrales M, Perri D, Robesti D, Tsaturyan A, Somani BK, Kartalas Goumas I, Traxer O, Ventimiglia E (2025) Intrarenal Fluid Temperature During Laser Lithotripsy: A Mini Review by the European Association of Urology Endourology Section. Eur Urol Focus. ;11(5):721–724. doi: 10.1016/j.euf.2025.05.009. Epub 2025 Jun 4. PMID: 40473536
3. Pauchard F, Ventimiglia E, Corrales M, Traxer O (2022) A Practical Guide for Intra-Renal Temperature and Pressure Management during RIRS: What Is the Evidence Telling Us. J Clin Med 11:3429. 10.3390/jcm11123429
4. Tokas T, Tzanaki E, Nagele U, Somani BK (2021) Role of Intrarenal Pressure in Modern Day Endourology (Mini-PCNL and Flexible URS): a Systematic Review of Literature. Curr Urol Rep 22:52. 10.1007/s11934-021-01067-5
5. Dean NS, Krambeck AE (2023) Endourologic Procedures of the Upper Urinary Tract and the Effects on Intrarenal Pressure and Temperature. J Endourol 37:191–198. 10.1089/end.2022.0630
6. Jahrreiss V, Nedbal C, Castellani D, Gauhar V, Seitz C, Zeng G, Juliebø-Jones P, Keller E, Tzelves L, Geraghty R, Rangarajan K, Traxer O, Philip J, Skolarikos A, Kallidonis P, Bres-Niewada E, Somani B (2024) Is suction the future of endourology? Overview from EAU Section of Urolithiasis. Ther Adv Urol 16:17562872241232275. 10.1177/17562872241232275. PMID: 38405421; PMCID: PMC10893777
7. Gauhar V, Traxer O, Castellani D, Sietz C, Chew BH, Fong KY, Hamri SB, Gökce MI, Gadzhiev N, Galosi AB, Yuen SKK, El Hajj A, Ko R, Zawadzki M, Sridharan V, Lakmichi MA, Corrales M, Malkhasyan V, Ragoori D, Soebhali B, Tan K, Chai CA, Tursunkulov AN, Tanidir Y, Persaud S, Elshazly M, Kamal W, Tefik T, Shrestha A, Tiong HC, Somani BK (2024) Could Use of a Flexible and Navigable Suction Ureteral Access Sheath Be a Potential Game-changer in Retrograde Intrarenal Surgery? Outcomes at 30 Days from a Large, Prospective, Multicenter, Real-world Study by the European Association of Urology Urolithiasis Section. Eur Urol Focus 10(6):975–982. 10.1016/j.euf.2024.05.010. Epub 2024 May 24. PMID: 38789313
8. Nedbal C, Gauhar V, Yuen SKK, Castellani D, Herrmann T, Traxer O, Somani BK (2025) Quadrifecta during retrograde intrarenal surgery: suction, irrigation, intrarenal temperature and pressure: achieving best clinical outcomes - an overview from EAU Endourology. Ther Adv Urol 17:17562872251335268 PMID: 40309358; PMCID: PMC12041686
9. Lee H, Elises JCR, Lee GM, Lee JH, So SW, Castillo CJ et al (2026) Laser, irrigation, and suction settings to optimize intra-renal temperature and pressure during automated laser lithotripsy in an ex vivo study part I. Sci Rep 16:1981. 10.1038/s41598-025-25265-0
10. Gauhar V,b;, Somani B,c;, Kwok (2026) Jia-Lunb,d,e; Yuen, Steffi Kar Keib,f. Paradigm shifts in fluid management using suction irrigation pressure autoregulating systems in modern flexible ureteroscopy with flexible and navigable suction access sheath: an evidence-based narrative from EAU Endourology. Current Opinion in Urology ():10.1097/MOU.0000000000001411, May 15, | 10.1097/MOU.0000000000001411
11. Hein S, Petzold R, Schoenthaler M, Wetterauer U, Miernik A (2018) Thermal effects of Ho: YAG laser lithotripsy: real-time evaluation in an in vitro model. World J Urol 36:1469–1475. 10.1007/s00345-018-2303-x
12. Okhunov Z, Jiang P, Afyouni AS, Ayad M, Arada R, Brevik A et al (2021) Caveat Emptor: The Heat Is ON-An In Vivo Evaluation of the Thulium Fiber Laser and Temperature Changes in the Porcine Kidney During Dusting

and Fragmentation Modes. J Endourol 35:1716–1722. 10.1089/end.2021.0206

13. Jianghua Yang Z, Li C, Lai K, Xu A (2024) In Vivo Assessment of a Novel Temperature Control Flexible Ureteroscope System for Monitoring and Controlling Intrarenal Temperature During Flexible Ureteroscopy, Urology, Volume 191, Pages 38–44, ISSN 0090-4295, https://doi.org/10.1016/j.urology.2024.07.011. (https://www.sciencedirect.com/science/article/pii/S0090429524005661)
14. Aldoukhi AH, Dau JJ, Majdalany SE, Hall TL, Ghani KR, Hollingsworth JM, Ambani SN, Dauw CA, Roberts WW (2021) Patterns of Laser Activation During Ureteroscopic Lithotripsy: Effects on Caliceal Fluid Temperature and Thermal Dose. J Endourol 35(8):1217–1222. 10.1089/end.2020.1067. Epub 2021 Feb 3. PMID: 33397188; PMCID: PMC8670574
15. Petzold R, Suarez-Ibarrola R, Miernik A (2021) Temperature Assessment of a Novel Pulsed Thulium Solid-State Laser Compared with a Holmium:Yttrium-Aluminum-Garnet Laser. J Endourol 35:853–859. 10.1089/end.2020.0803
16. Peng Y, Liu M, Ming S, Yu W, Li L, Lu C et al (2020) Safety of a Novel Thulium Fiber Laser for Lithotripsy: An In VitroStudy on the Thermal Effect and Its Impact Factor. J Endourol 34:88–92. 10.1089/end.2019.0426
17. Winship B, Wollin D, Carlos E, Peters C, Li J, Terry R et al (2019) The Rise and Fall of High Temperatures During Ureteroscopic Holmium Laser Lithotripsy. J Endourol 33:794–799. 10.1089/end.2019.0084
18. Wei Zhu S, Liu J, Cao H, Wang H, Liang K, Jiang Y, Cui CA, Chai EB, Sahinler A, Aquino G, Mazzon W, Zhong Z, Zhao L, Zhang J, Ding Q, Wang Y, Wang KW, Chen Y, Liu S, Choong K, Sarica (2024) Guohua Zeng,Tip bendable suction ureteral access sheath versus traditional sheath in retrograde intrarenal stone surgery: an international multicentre, randomized, parallel group, superiority study, eClinicalMedicine. 74(102724):2589–5370. https://doi.org/10.1016/j.eclinm.2024.102724
19. Cabo J, Ballantyne C, Edmonds V, Stern KL (2025) Laser Lithotripsy Strategies: Fragmenting, Popcorning, Dusting, and How Intrarenal Pressure Should Be Considered. Urol Clin North Am 52:375–389. 10.1016/j.ucl.2025.04.004

Figures

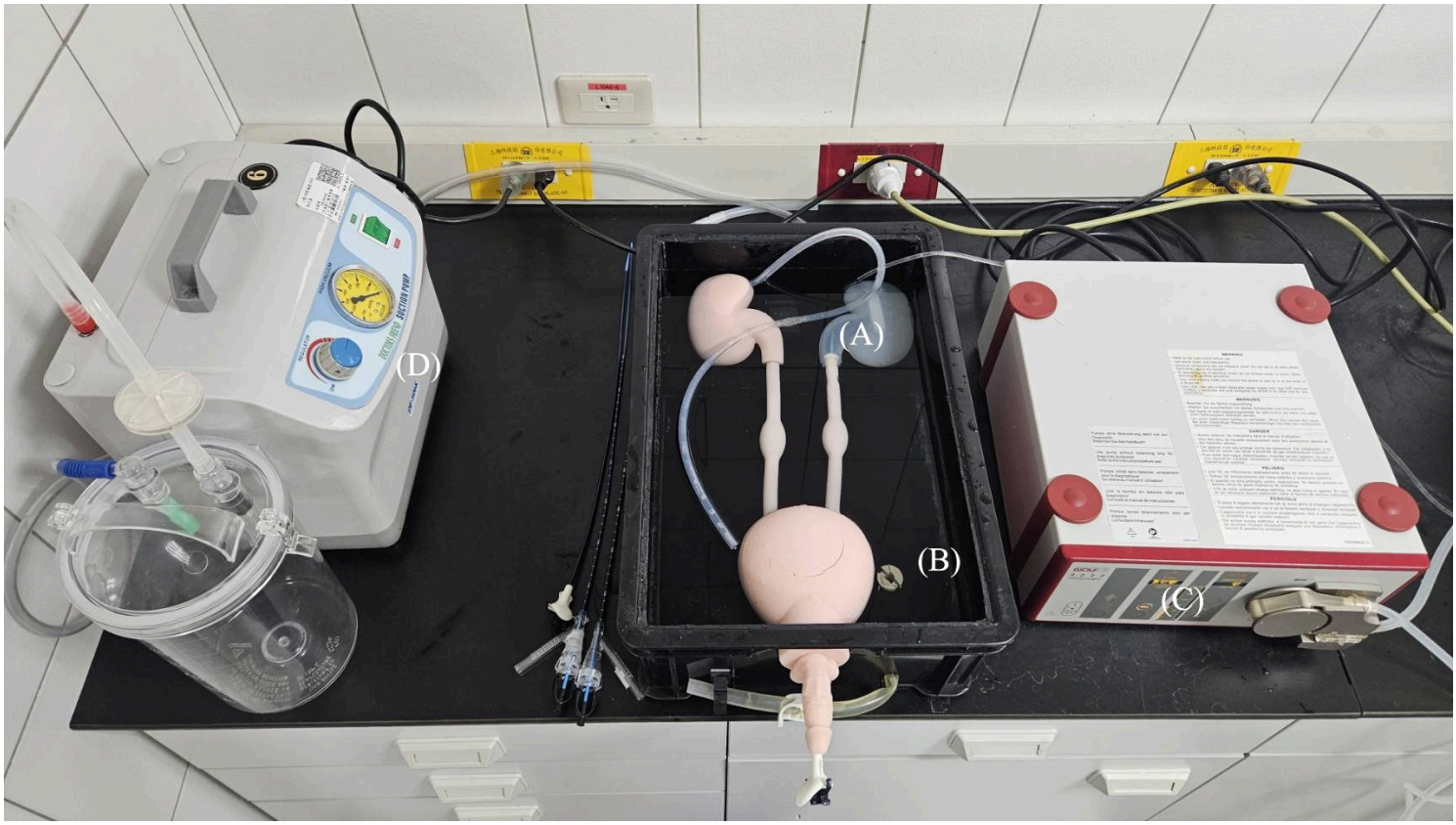


Figure 1

In vitro experimental setup for simultaneous intrarenal pressure and temperature assessment.
A silicone kidney–ureter–bladder model (A) was placed in a water-filled container (B). Fixed irrigation was provided by an irrigation machine (C) positioned on the right side of the setup, while suction was generated by a suction pump (D) positioned on the left side.

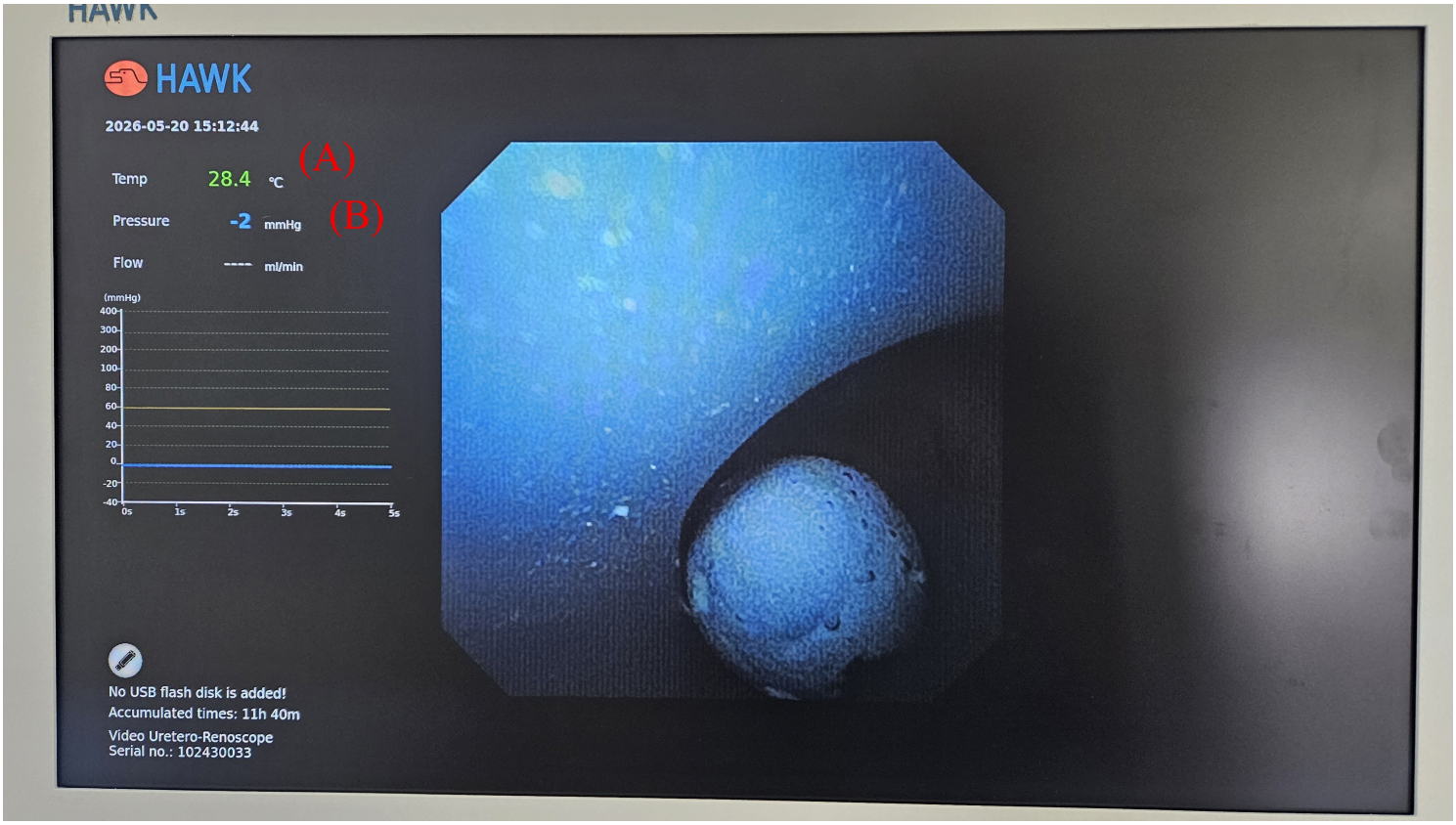


Figure 2

Real-time monitoring of intrarenal temperature and pressure.
IRT (A)and IRP (B) were continuously recorded during the experiment, and real-time measurements (C) were displayed on the monitor throughout laser activation.
*IRT= intrarenal temperature; IRP= intrarenal pressure

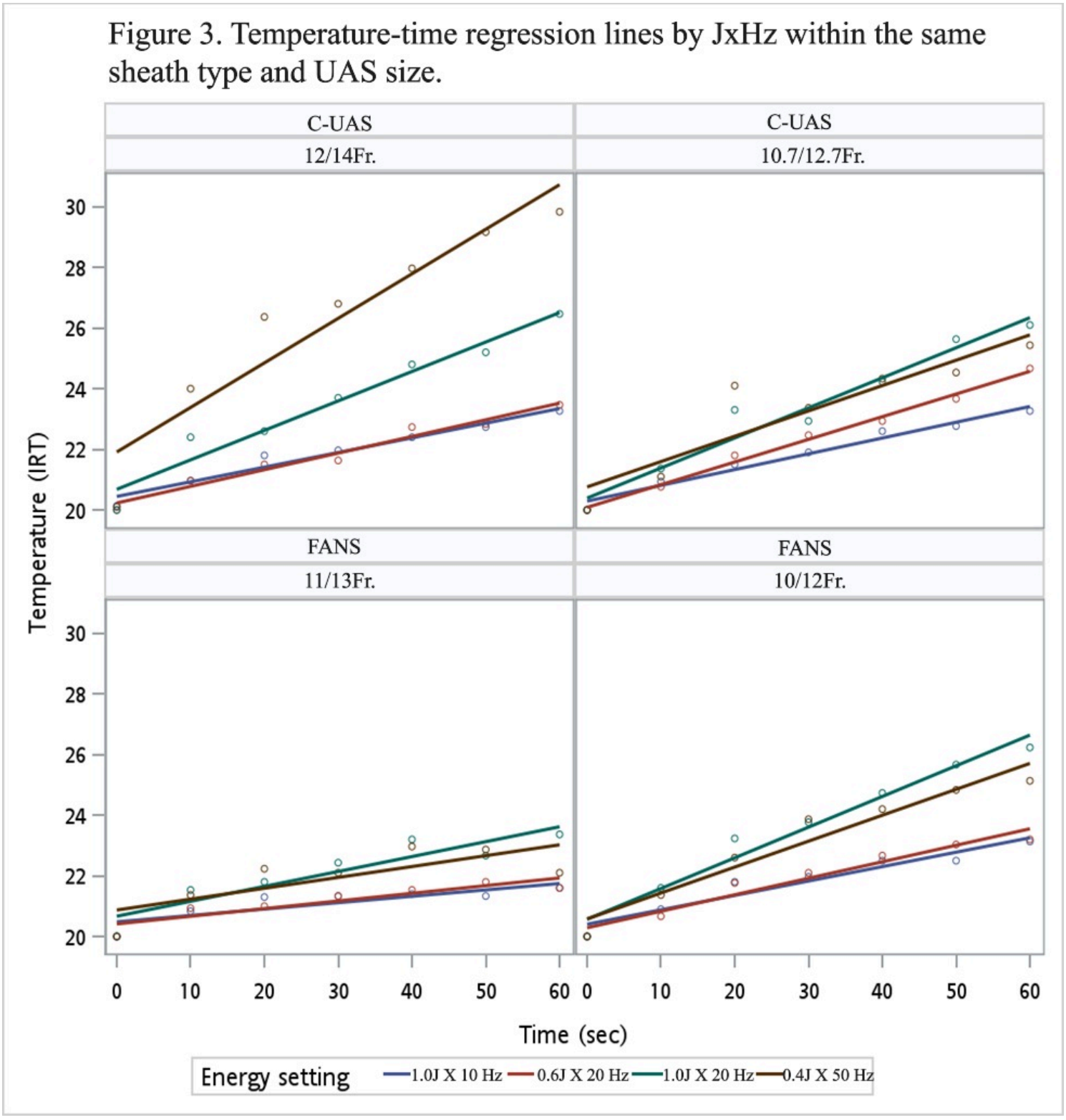


Figure 3

Temperature-time regression lines by JxHz within the same sheath type and UAS size.
IRT values are shown as scatter points, and fitted linear regression lines are shown for each JxHz laser setting. Panels are stratified by C-UAS or FANS and UAS size. This figure shows the temperature-time trends among different laser settings under the same sheath type and UAS size condition.

*C-UAS = conventional UAS; FANS = Flexible and Navigable Suction sheath; UAS=Ureteral access sheath; IRT= intrarenal temperature

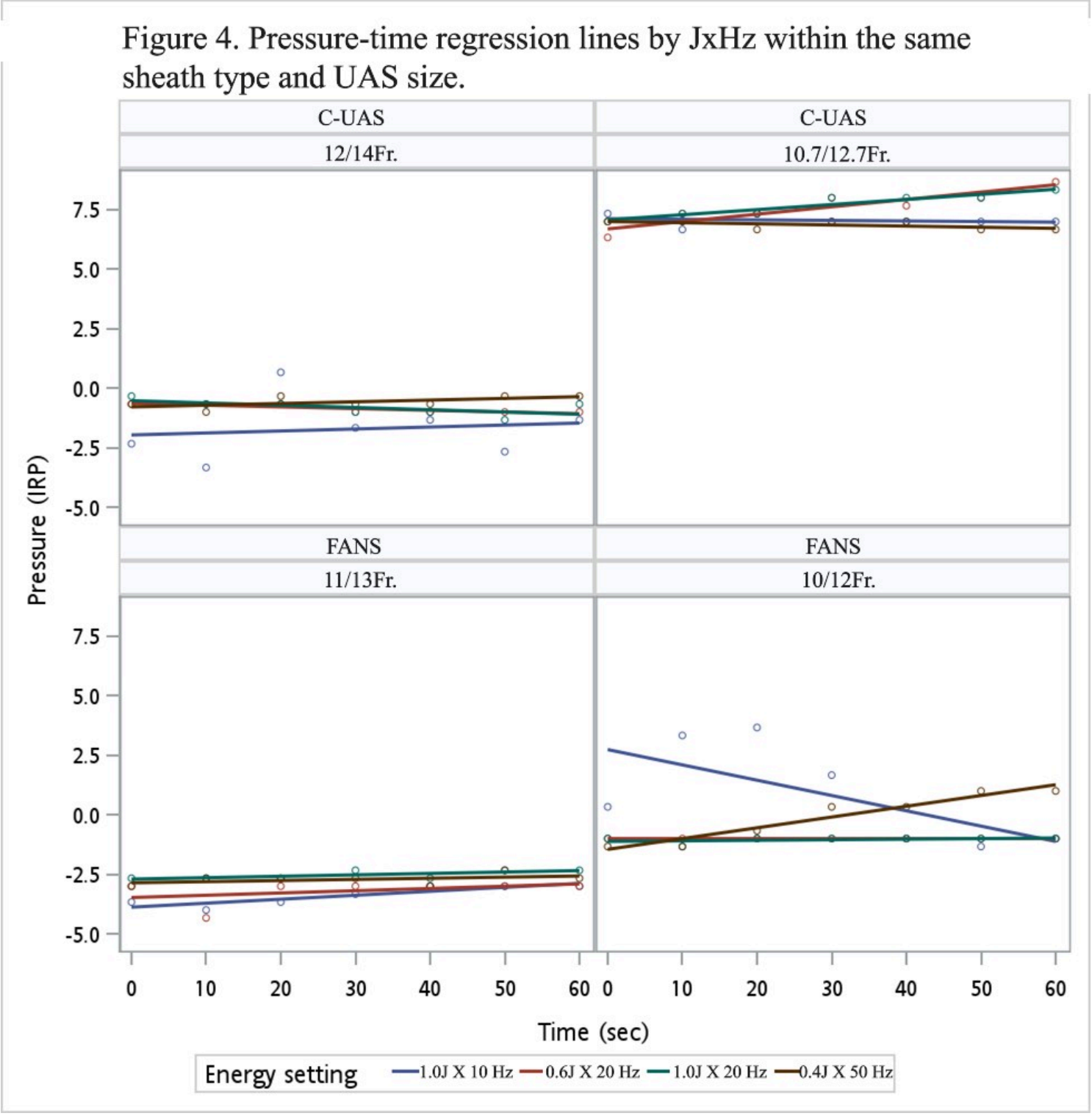


Figure 4

Pressure-time regression lines by JxHz within the same sheath type and UAS size.
Observed IRP values are shown as scatter points, and fitted linear regression lines are shown for each JxHz laser setting. Panels are stratified by C-UAS or FANS and UAS size. This figure shows the pressure-time trends among different laser settings under the same sheath type and UAS size condition.

*C-UAS = conventional UAS; FANS = Flexible and Navigable Suction sheath; UAS=Ureteral access sheath; IRP= intrarenal pressure

Supplementary Files

This is a list of supplementary files associated with this preprint. Click to download.

- SupplementaryFigure1.png
- SupplementaryFigure2.png
- SupplementaryFigure3.png
- SupplementaryFIgure4.png